Journal of Coordination Chemistry
Publication details, including instructions for authors and subscription information:
http://www.tandfonline.com/loi/gcoo20

Synthesis, crystal structure, and DNA interaction of an oxovanadium(IV) complex containing L-valine Schiff base and 1,10-phenanthroline

Buqin Jing [a b], Jianfang Dong [b c], Jinghong Li [b], Tao Xu [b] & Lianzhi Li [b]

[a] College of Chemistry and Chemical Engineering, Shanxi Datong University, Datong, Shanxi, P.R. China

[b] Shandong Provincial Key Laboratory of Chemical Energy Storage and Novel Cell Technology, School of Chemistry and Chemical Engineering, Liaocheng University, Liaocheng, P.R. China

[c] Department of Material Science, Shandong Polytechnic Technician College, Liaocheng, Shandong, P.R. China

Accepted author version posted online: 18 Jan 2013.Published online: 20 Feb 2013.

To cite this article: Buqin Jing, Jianfang Dong, Jinghong Li, Tao Xu & Lianzhi Li (2013) Synthesis, crystal structure, and DNA interaction of an oxovanadium(IV) complex containing L-valine Schiff base and 1,10-phenanthroline, Journal of Coordination Chemistry, 66:3, 520-529, DOI: 10.1080/00958972.2013.763939

To link to this article: http://dx.doi.org/10.1080/00958972.2013.763939

Journal of Coordination Chemistry
Vol. 66, No. 3, 10 February 2013, 520–529

Synthesis, crystal structure, and DNA interaction of an oxovanadium(IV) complex containing L-valine Schiff base and 1,10-phenanthroline

BUQIN JING†,‡, JIANFANG DONG‡,§, JINGHONG LI‡, TAO XU‡ and LIANZHI LI*‡

‡College of Chemistry and Chemical Engineering, Shanxi Datong University, Datong, Shanxi, P.R. China
‡Shandong Provincial Key Laboratory of Chemical Energy Storage and Novel Cell Technology, School of Chemistry and Chemical Engineering, Liaocheng University, Liaocheng, P.R. China
§Department of Material Science, Shandong Polytechnic Technician College, Liaocheng, Shandong, P.R. China

(*Received 7 September 2012; in final form 23 October 2012*)

A new oxovanadium(IV) complex, $[VO(sal\text{-}val)(phen)]\cdot CH_3OH\cdot H_2O$ (sal-val = Schiff base derived from salicylaldehyde and L-valine, phen = 1,10-phenanthroline), has been synthesized and characterized by elemental analysis, IR spectra, and single-crystal X-ray diffraction. This crystal belongs to monoclinic crystal system, *C2/c* space group with crystallographic data: $a = 28.031(4)$ Å, $b = 9.342(3)$ Å, $c = 19.198(4)$ Å, $\beta = 99.425(2)°$, and $Z = 8$. The V^{IV} was six-coordinate to form an octahedral geometry. In the crystal, intermolecular hydrogen bonding and π–π stacking formed the 1-D network. DNA-binding properties of this oxovanadium(IV) complex with calf-thymus DNA (CT-DNA) were investigated using UV, fluorescence, and circular dichroism spectra. The complex can bind to CT-DNA via intercalation.

Keywords: Oxovanadium(IV) complex; L-valine; Schiff base; DNA interaction

1. Introduction

Studying interaction of small molecules with DNA attracts attention for importance in cancer therapy and molecular biology [1,2]. Transition metal complexes have been used, because by changing the ligand environment, one can tune the DNA binding and cleaving ability of a metal complex [3]. Vanadium complexes have shown biological and pharmacological properties [4,5]. Because of low toxicity of VO(IV), some vanadium complexes have been isolated, characterized, and tested for biological activity [6,7]. Furthermore, oxovanadium complexes, especially with phenanthroline or its derivative ligands, exhibit potent antitumor activity [8], DNA binding and DNA-photocleavage activities [9,10].

*Corresponding author. Email: lilianzhi@lcu.edu.cn

ISSN 0095-8972 print/ISSN 1029-0389 online
http://dx.doi.org/10.1080/00958972.2013.763939

Schiff base complexes play an important role as models, with easy preparation, diversity, and structural variation [11]. Schiff base complexes also have wide applications in medicine, biochemical reactions, and biological regulators [12–14]. Amino acids and their derivatives are important for their roles in biochemical reactions. Efforts have been made to synthesize and characterize amino Schiff base complexes with transition metals [15,16]. Compared with other transition metal Schiff base complexes, vanadium complexes are less studied. We have synthesized and structurally characterized several oxovanadium complexes with mixed ligands of multidentate Schiff base and 1,10-phenanthroline [17–21]. To continue our research, we have synthesized and characterized a new oxovanadium(IV) complex containing L-valine Schiff base and 1,10-phenanthroline. The DNA-binding properties of this complex have been investigated by UV–Vis absorption, fluorescence, and circular dichroism (CD) spectra.

2. Experimental

2.1. *Materials*

Salicylaldehyde was purchased from Alfa Aesar. L-valine was obtained from Beijing Jingke Company. Calf-thymus DNA (CT-DNA) and ethidium bromide (EB) were obtained from Sigma Chemical Co. All other reagents were of analytical grade or biochemical quality. All the measurements involving the interactions of this oxovanadium(IV) complex were carried out in doubly distilled water buffer containing 10 mmol L^{-1} Tris-HCl/10 mmol L^{-1} NaCl (pH 7.1). Solution of CT-DNA in the buffer gave a ratio of UV absorbance at 260 and 280 nm (A_{260}/A_{280}) of 1.8–1.9, indicating that the DNA was sufficiently pure and free of protein [22]. The DNA concentration per nucleotide was determined by absorption spectroscopy using the molar absorption coefficient (6600 (mol L^{-1})$^{-1}$cm^{-1}) at 260 nm [23].

2.2. *Physical measurement*

Elemental analyzes for C, H, and N were performed on a Perkin-Elmer 2400 II analyzer. IR spectrum was obtained with KBr pellets on a Nicolet 5700 FT-IR from 4000 to 400 cm^{-1}. UV–Vis absorption spectra were recorded on a Hewlett-Packard HP-8453A diode array spectrophotometer. Fluorescence spectra were recorded on a LS55 spectrofluorometer. CD spectral measurements were conducted on a Jasco J-810 spectropolarimeter.

2.3. *Synthesis of [VO(sal-val)(phen)]·CH_3OH·H_2O*

L-valine (0.117 g, 1 mmol) and potassium hydroxide (0.056 g, 1 mmol) were dissolved in hot methanol (10 mL) and added in portions to a methanol solution (5 mL) of salicylaldehyde (1 mmol, 0.11 mL). The mixture was then stirred at 323 K for 2 h. Subsequently, an aqueous solution (3 mL) of vanadyl sulfate hydrate (0.225 g, 1 mmol) was added dropwise and stirred for 2 h. A methanol solution (5 mL) of 1,10-phenanthroline (0.198 g, 1 mmol) was added dropwise and stirred for an additional 4 h. The resultant solution was filtered and held at room temperature for ten days, whereupon brown crystals suitable for X-ray diffraction were obtained. Yield: 78%. m.p. 315–317 °C. Anal. Calcd for $C_{25}H_{27}N_3O_6V$ (%): C,

58.14; H, 5.27; N, 8.13. Found (%): C, 58.36; H, 5.39; N, 7.91%. IR (KBr, ν/cm^{-1}): 3418 (ν_{O-H}), 1643($\nu_{C=N}$), 1621($\nu_{C=N}$), 848, 728($\nu_{C=Nphen}$), 960($\nu_{V=O}$).

2.4. *X-ray crystallography*

A crystal was mounted in a glass capillary and data were collected on a Bruker Smart-1000 CCD area-detector with graphite monochromated Mo Kα radiation ($\lambda = 0.71073$ Å). A semi-empirical absorption correction was applied to the data. The structure was solved by direct methods using SHELXLS-97 and refined against F^2 by full matrix least squares using SHELXL-97 [24,25]. Hydrogens were placed in calculated positions. A summary of pertinent crystal data, experimental details and refinement results are shown in table 1.

2.5. *DNA-binding experiments*

All DNA-binding experiments were carried out in 10 mmol L^{-1} Tris-HCl/10 mmol L^{-1} NaCl, pH 7.1 buffer solutions. UV–Vis absorption spectra were recorded by varying complex concentration in the buffer solution while keeping CT-DNA concentration constant. Correction was made for absorbance of the complex itself. DNA-complex solutions were incubated for 1 h before absorption spectra were recorded.

For fluorescence quenching experiments, the oxovanadium(IV) complex was added to CT-DNA solution treated with EB for 30 min in the buffer solution. All samples were excited at 340 nm, and emission spectra were recorded at 550–650 nm. Each spectrum was

Table 1. Crystal data and structure refinement for the complex.

Empirical formula	$C_{25}H_{27}N_3O_6V$
Formula weight	516.44
Temperature (K)	298(2)
Wavelength (Å)	0.71073
Crystal system	Monoclinic
Space group	*C2/c*
Unit cell dimensions	
a (Å)	28.031(4)
b (Å)	9.342(3)
c (Å)	19.198(4)
α(°)	90
β(°)	99.425(2)
γ(°)	90
Volume (Å^3)	4959.3(18)
Z	8
Dcalc (Mg m^{-3})	1.383
Absorption coefficient (mm^{-1})	0.445
F (000)	2152
Crystal size (mm)	0.48 × 0.42 × 0.09
θ Range for data collection (°)	2.15–25.02
Limiting indices	−26,33; −11,10; −22,22
Reflections collected/unique	12,610/4367
R(int)	0.0423
Data/restraints/parameters	4367/2/317
Goodness-of-fit of F^2	1.023
Final *R* indices [$I > 2\sigma(I)$]	$R_1 = 0.0432$, w$R_2 = 0.0997$
R indices (all data)	$R_1 = 0.0730$, w$R_2 = 0.1181$
Largest diff. peak and hole (e A^{-3})	0.410 and –0.260

recorded at a scan speed of 200 nm min^{-1} and slit width of 7 nm for both excitation and emission monochromators.

CD spectra of CT-DNA were carried out on a J-810 spectropolarimeter at room temperature with a quartz cell of 1 cm pathlength by increasing complex/CT-DNA ratio ($r = 0$, 0.4, 0.8, 1.2, 1.6, and 2.0) in the buffer. Each sample solution was scanned from 220 to 320 nm with a scan speed of 100 nm min^{-1} and 1 s response time. Each spectrum was obtained after three accumulations from which the buffer background had been subtracted.

3. Results and discussion

3.1. *Infrared spectra*

IR spectra of the complex showed moderate absorption at 960 cm^{-1} assigned to V=O stretch. The very sharp absorption at 1644 cm^{-1} was characteristic vibration of the imine (C=N) in the complex. Weak bands at 848 and 728 cm^{-1} are attributed to ring-stretching frequencies [ν(C=C) and ν(C=N)] of 1,10-phenanthroline. Two moderate absorptions at 1621 and 1385 cm^{-1} were assigned to asymmetric and symmetric stretches of CO_2^-, respectively [26]. The frequency separation ($\Delta\upsilon$) is greater than 200 cm^{-1}, suggesting monodentate carboxyl group [27].

3.2. *Structure description*

The molecular structure of $[VO(sal\text{-}val)(phen)]\cdot CH_3OH\cdot H_2O$ with atom-numbering scheme is depicted in figure 1. Principal bond lengths and angles of this complex are listed in table 2. The oxovanadium(IV) coordinated with tridentate Schiff base derived from condensation of salicylaldehyde and L-valine, and 1,10-phenanthroline. The V(IV) was

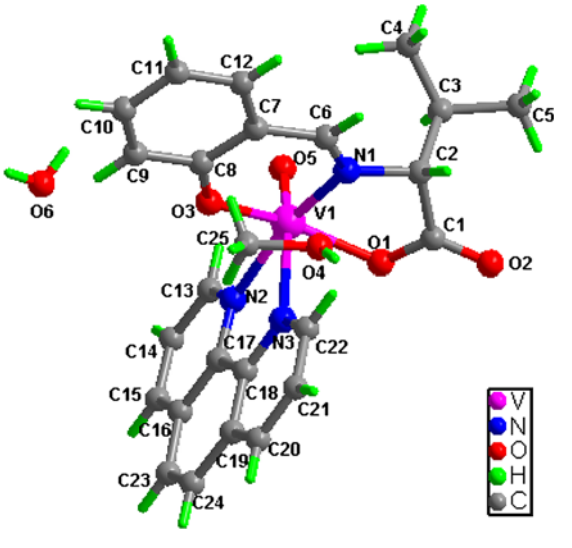

Figure 1. The molecular structure of the title complex with atom-numbering scheme.

Table 2. Selected bond lengths (Å) and angles (°) for the complex.

V1–O5	1.600(2)
V1–O3	1.937(2)
V1–O1	2.007(2)
V1–N1	2.047(2)
V1–N2	2.147(2)
V1–N3	2.364(2)
O5–V1–O3	103.57(11)
O5–V1–O1	101.13(10)
O3–V1–O1	154.12(9)
O5–V1–N1	102.38(10)
O3–V1–N1	88.49(8)
O1–V1–N1	78.76(9)
O5–V1–N2	93.03(10)
O3–V1–N2	91.14(8)
O1–V1–N2	95.16(8)
N1–V1–N2	164.23(9)
O5–V1–N3	165.70(10)
O3–V1–N3	78.23(9)
O1–V1–N3	79.75(8)
N1–V1–N3	91.81(9)
N2–V1–N3	72.70(8)

six-coordinate in distorted octahedral geometry by one terminal oxygen (O5), two oxygens (O1, O3), and one nitrogen (N1) from the amino acid Schiff base, and two nitrogens (N2, N3) from 1,10-phenanthroline. The terminal oxo O5 and N3 occupy axial positions with *trans* angle of 165.70(10)°. O1, O3, and N1 of the tridentate Schiff base and N2 of 1,10-phenanthroline form the equatorial plane. The deviations of V1, O5, and N3 out of the equatorial plane were 0.3459(12) Å, 1.9400(24) Å, and −1.9849(27) Å, indicating that vanadium was displaced toward oxo O5 with V1=O5 bond length 1.600(2) Å. The V1–N3 bond distance of 2.364(2) Å *trans* to V1=O5 is considerably longer than V–N bonds in the equatorial plane. The tridentate Schiff base coordinated to vanadium formed two basal chelated planes. The dihedral angle between the O1–C1–C2–N1–V1 plane and the N1–C6–C7–C8–O3–V1 plane was 18.14(11)°. Phenanthroline coordinated to V1 in the direction almost vertical to the equatorial plane, which formed the dihedral angle 86.94(5)°.

There are abundant intra- and intermolecular hydrogen bonds in the crystal structure. Hydrogen bond lengths and angles are listed in table 3. The intermolecular O4−H5−O6^{i} (i = x, 1−y, z−0.5) and O6−H26···O4^{ii} (ii = 0.5−x, 0.5−y, 1−z) hydrogen bonds formed between solvent water and methanol. Thus, these intermolecular hydrogen bonds and the complementary intermolecular hydrogen bond O6−H27···O2^{iii} (iii = x, y, z + 1) linked

Table 3. Hydrogen bond lengths (Å) and angles (°) of the complex.

D−H···A	*d*(D−H)	*d*(H−A)	*d*(D−A)	∠(DHA)
C5−H5a···O2	0.96	2.48	3.158(5)	127.2
C13−H13···O5	0.93	2.52	2.987(4)	111.2
O4−H5···O6^{i}	0.82	2.21	2.703(4)	119.3
O6−H26···O4^{ii}	0.85	1.95	2.796(4)	176.9
O6−H27···O2^{iii}	0.85	1.96	2.806(3)	170.6
C13−H13···O5^{iv}	0.93	2.52	3.256(4)	136.7

Note: Symmetry codes: i = *x*, 1 − *y*, *z* − 0.5; ii = 0.5 − *x*, 0.5 − *y*, 1 − *z*; iii = *x*, *y*, *z* + 1, iv = 1 − *x*, −*y*, −*z*.

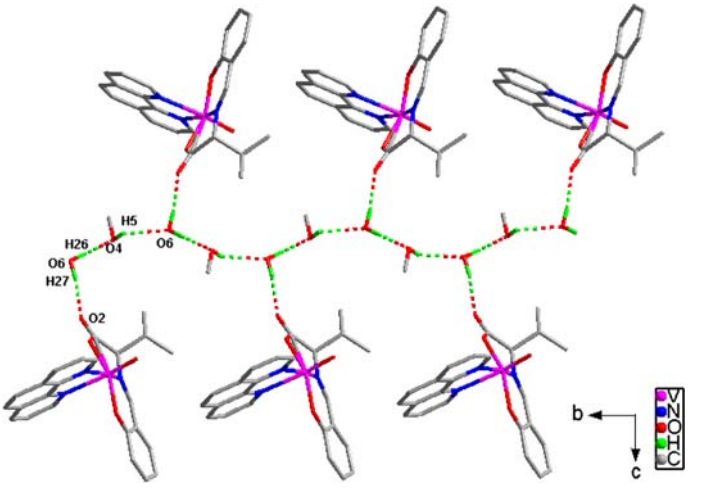

Figure 2. 1D hydrogen-bonded packing diagram of the complex; hydrogen bonding is represented by dashed line.

together to form a 1-D supramolecular structure along the *b*-axis in the *bc*-plane (figure 2). As shown in figure 3, a dimer was formed between molecules through C13−H13···O5^{iv} (iv = 1−x, −y, −z) hydrogen bond interactions. The intramolecular C−H···O interaction was formed by C5−H5a···O2 and C13−H13···O5, which stabilized the crystal structure along with the intermolecular hydrogen bonds. Inner connectivity occurred among the dimers *via* π–π interaction involving phenanthroline having centroid-centroid separation of 3.613 Å [28,29].

3.3. *DNA-binding studies*

3.3.1. Electronic absorption spectral studies. "Hyperchromic effect" and "hypochromic effect" are spectral features of DNA concerning its double-helix structure. This spectral change process reflects corresponding changes of DNA in its conformation and structure

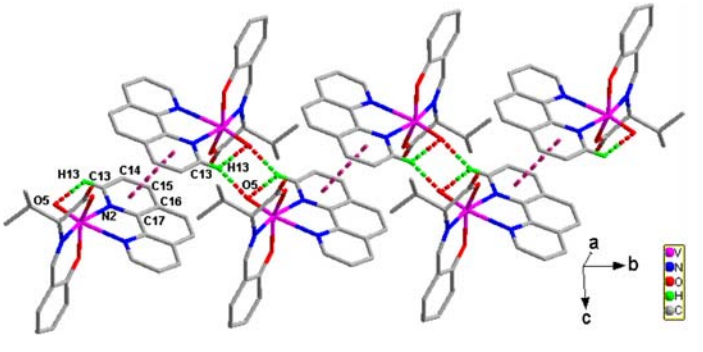

Figure 3. 1D packing diagram by hydrogen bond and π–π interaction of the complex; the hydrogen bond and π–π interaction are drawn in dashed line.

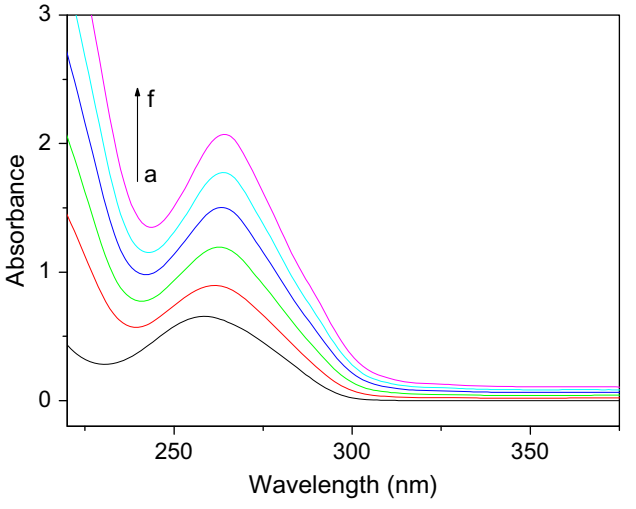

Figure 4. Electronic absorption spectra of CT-DNA (1.5×10^{-4} mol L^{-1}) in the absence (a) and presence (b–f) of the complex at ratios of [complex]/[DNA] (b–f) = 3, 6, 9, 12, 15.

because of the interaction of the complex with DNA. Hypochromism results from the contraction of DNA in the helix axis, while hyperchromism results from damage of the DNA double-helix structure [30]. When this vanadium complex at various concentrations was added to DNA solution, changes of the electronic absorption spectra are shown in figure 4. The absorption spectra of DNA at 260 nm increased gradually accompanying a red-shift upon increasing the vanadium complex concentrations. This typical hyperchromic effect may be because the purine bases and pyrimidine bases of DNA were exposed because of the binding of the complex to DNA [31], causing the slight change of conformation of CT-DNA [32]. The observed bathochromism is evidence of stabilization of the CT-DNA duplex [33], while the existence of intercalative binding may not be ruled out [34].

3.3.2. Fluorescence spectral studies. Fluorescence measurements for this oxovanadium (IV) complex showed no emission band whether with or without CT-DNA at ambient temperature in aqueous solution. To further investigate the interaction of this complex with DNA, a competitive binding experiment using EB as a probe was carried out [35]. The extent of fluorescence quenching of EB-DNA system is used to determine the extent of binding of other molecules to DNA. As shown in figure 5, the addition of the complex to DNA pretreated with EB caused appreciable reduction in the emission intensity, indicating that this complex could partially displace EB from the DNA-EB system, as often observed in intercalative complex-DNA mode [36].

To evaluate the binding strength of this oxovanadium(IV) complex to CT-DNA, the Stern–Volmer constant K_{sq} was obtained from the linear Stern–Volmer equation [37]: $I_0/I = 1 + K_{sq}r$, where I_0 and I are fluorescence intensities in the absence and presence of the vanadium(IV) complex, respectively. K_{sq} is a linear Stern–Volmer constant and r is the concentration ratio of the complex to DNA. The K_{sq} value obtained from the ratio of slope and intercept obtained from the plot of I_0/I versus r (figure 6) is 1.03. Such a value of quenching constant indicates that the interaction of the complex with DNA is weaker

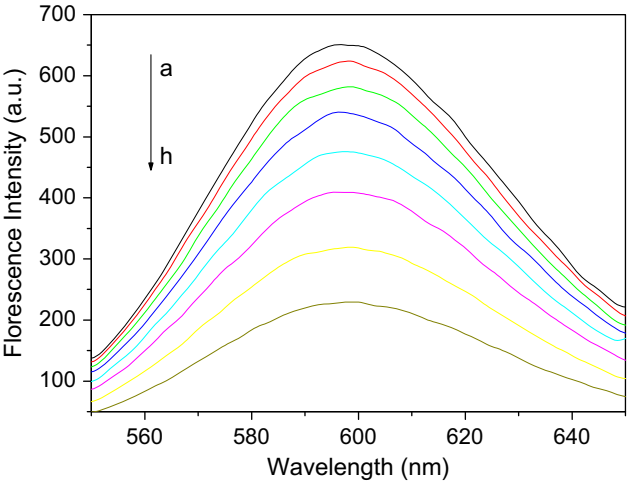

Figure 5. Fluorescence spectra of CT-DNA-EB system in the absence (a) and presence of the complex at ratios of [complex]/[DNA] (b–h) = 0, 0.1, 0.2, 0.4, 0.6, 0.8, 1.2, 2.0. [DNA] = 25 μmol L^{-1}, [EB] =3 μmol L^{-1}.

than those of {[VO(Naph-L-Tyr)(Phen)]·CH_3OH} (K_{sq} = 1.99) [20], [VO(Naph-Trp)(phen)]·CH_3OH (K_{sq} = 1.89), [VO(*o*-Van-Trp)(phen)]·$CH_3OH·H_2O$ (K_{sq} = 1.34) [38], [VO(satsc)(phen)], [VO(3,5-dibrsatsc)(phen)] [39], [VO(SAA)(phen)] and [VO(MOSAA)(phen)] [40]. The difference of DNA-binding ability among these complexes may come from the differences of their structures and steric hindrance of individual ligands.

3.3.3. Circular dichroism spectral studies. CD spectroscopy may give information on how the conformation of the CT-DNA is influenced by the complex. The B-form conformation of CT-DNA shows two CD bands in the UV region: a positive band at 275 nm due to base stacking and a negative band at 245 nm due to polynucleotide helicity [41,42]. The changes in CD signals of CT-DNA are often assigned to the corresponding changes in

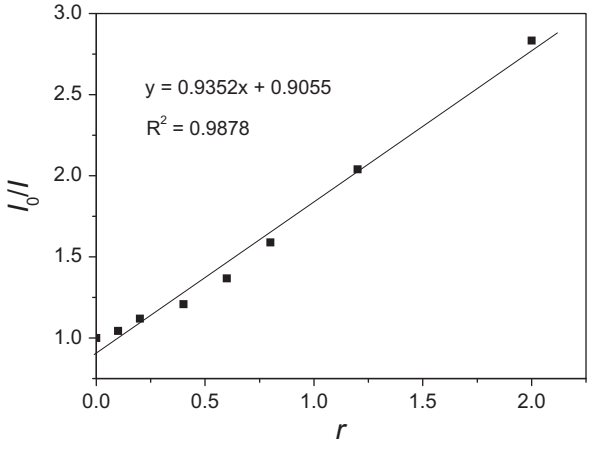

Figure 6. Stern–Volmer plot of I_0/I vs. r for the complex; r = [complex]/[DNA].

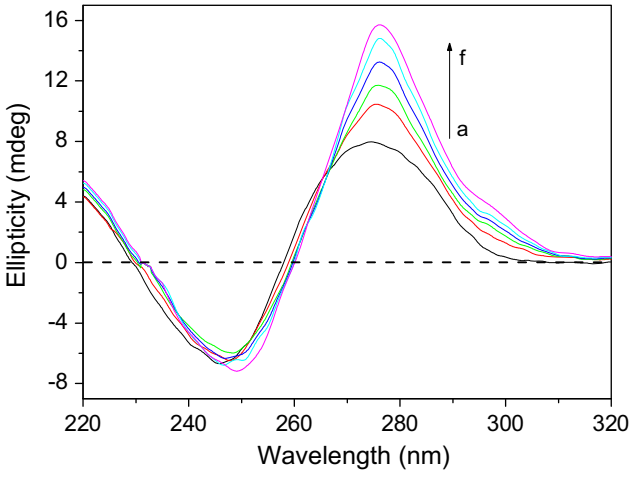

Figure 7. CD spectra of CT-DNA (100 μmol L^{-1}) in the absence (a) and presence of the complex at ratios of [complex]/[DNA](b–f) = 0.4, 0.8, 1.2, 1.6, 2.0.

CT-DNA structure [43]. Simple groove binding and electrostatic interaction of the complex with CT-DNA shows little or no perturbation on base stacking and helicity bands, whereas intercalation can enhance the intensities of both bands to stabilize the right-handed B conformation [42].

The CD spectra of CT-DNA showed a remarkable increase in the positive band in ellipticity with a red shift when the complex concentrations were increased (figure 7). When the ratio of [complex]/[DNA] reached 2.0, the positive maximum absorption had increased about 96.90% with a 1 nm red shift (figure 7). The observation supports intercalative binding for this complex. Insertion of the complex into adjacent base pairs prevents neighboring base pairs from close stacking, leading to an enhancement in the positive band [44]. These results suggest that CD spectra are closely correlated with fluorescence and electronic absorption spectra of DNA binding studies.

4. Conclusions

We have synthesized and characterized a new oxovanadium(IV) complex bearing a Schiff base derived from salicylaldehyde and L-valine, and 1,10-phenanthroline. DNA-binding experiments of this oxovanadium(IV) complex by UV, fluorescence and CD spectroscopy have been employed. All these results indicate that this complex binds to CT-DNA moderately in an intercalative mode. This study may be useful for evaluating and understanding those factors that determine the DNA-binding mode and cleavage mechanism of vanadium complexes.

Supplementary material

Detailed crystallographic data for the crystal structure analysis have been deposited with the Cambridge Crystallographic Data Center, CCDC No. 256,618. Copies of the information may be obtained free of charge from The Director, CCDC, 12 Union Road, Cambridge CB2 1EZ, UK (Fax: +44 1223 336,033; E-mail: deposit@ccdc.cam.ac.uk or www.ccdc.cam.ac.uk).

Acknowledgements

This project was supported by the Natural Science Foundation of Shandong Province of China (No. Y2004B02) and the Shandong Tai-Shan Scholar Research Found.

References

[1] E.L. Hegg, J.N. Burstyn. *Coord. Chem. Rev.*, **173**, 133 (1998).
[2] C.J. Burrows, J.G. Muller. *Chem. Rev.*, **98**, 1109 (1998).
[3] V. Uma, M. Kanthimathi, T. Weyhermuller, B.U. Nair. *J. Inorg. Biochem.*, **99**, 2299 (2005).
[4] H. Sakurai, Y. Kojima, Y. Yoshikawa, K. Kawabe, H. Yasui. *Coord. Chem. Rev.*, **226**, 187 (2002).
[5] H. Vilter. *Phytochemistry*, **23**, 1387 (1984).
[6] K.H. Thompson, C. Orvig. *Coord. Chem. Rev.*, **219–221**, 1033 (2001).
[7] E. Kiss, A. Bényei, T. Kiss. *Polyhedron*, **22**, 27 (2003).
[8] C. Djordjevic, G.L. Wampler. *J. Inorg. Biochem.*, **25**, 51 (1985).
[9] P.K. Sasmal, A.K. Patra, A.R. Chakravarty. *J. Inorg. Biochem.*, **102**, 1463 (2008).
[10] D.W.J. Kwong, O.Y. Chan, L.K. Shek, R.N.S. Wong. *J. Inorg. Biochem.*, **99**, 2062 (2005).
[11] A.D. Gamovski, A.L. Nivorozhkin, V.I. Minkin. *Coord. Chem. Rev.*, **126**, 1 (1993).
[12] N. Matsumoto, J.Z. Zhong, H. Okawa, S. Kida. *Inorg. Chim. Acta*, **160**, 153 (1989).
[13] D.C. Crans, A.D. Keramidas, H.H. Lity, O.P. Anderson, M.M. Miller, L.M. Lemoine, S.P. Williams, M. Vandenberg, A.J. Rossomando, L.J. Sweet. *J. Am. Chem. Soc.*, **119**, 5447 (1997).
[14] R.C. Burrous, J.C. Bailar. *J. Am. Chem. Soc.*, **88**, 4150 (1996).
[15] B.G. Kalagouda, S.P. Manjula, S.V. Ramesh, V.S. Rashmi, A.P. Siddappa. *Transition Met. Chem.*, **31**, 580 (2006).
[16] R.-M. Wang, C.-J. Hao, Y.-P. Wang, S.-B. Li. *J. Mol. Catal. A: Chem.*, **147**, 173 (1999).
[17] L.Z. Li, Z.H. Guo, Q.F. Zhang, T. Xu, D.Q. Wang. *Inorg. Chem. Commun.*, **13**, 1166 (2010).
[18] T. Xu, L.Z. Li, S.F. Zhou, G.Q. Guo, M.J. Niu. *J. Chem. Crystallogr.*, **35**, 263 (2005).
[19] L.Z. Li, B.Q. Jing, L.W. Li, T. Xu. *Z. Krist.-New Cryst. S.*, **221**, 1267/1907 (2006).
[20] L. Bian, L.Z. Li, Q.F. Zhang, H.L. Liu, D.Q. Wang. *Acta Chim. Sinica*, **69**, 1661 (2011).
[21] Z. Guo, L. Li, T. Xu, J. Li. *Acta Cryst. E*, **65**, m1114 (2009).
[22] J. Marmur. *J. Mol. Biol.*, **3**, 208 (1961).
[23] M.E. Reichmann, S.A. Rice, C.A. Thomas, P. Doty. *J. Am. Chem. Soc.*, **76**, 3047 (1954).
[24] G.M. Sheldrick. *SHELXS-97 Program for Crystal Structural Solution*, University of Göttingen, Göttingen (1997).
[25] G.M. Sheldrick. *SHELXL-97 Program for Crystal Structural Refinement*, University of Göttingen, Göttingen (1997).
[26] J. Vančo, J. Marek, Z. Trávníček, E. Račanská, J. Muselík, O. Švajlenová. *J. Inorg. Biochem.*, **102**, 595 (2008).
[27] M.A. Neelakantan, F. Rusalraj, J. Dharmaraja, S. Johnsonraja, T. Jeyakumar, M.S. Pillai. *Spectrochim. Acta Part A*, **71**, 1599 (2008).
[28] M.L.Tong, H.K. Lee, X.M. Chen, R.B. Huang, T.C.W. Mak. *J. Chem. Soc., Dalton Trans.*, 3657 (1999).
[29] C. Janiak. *J. Chem. Soc., Dalton Trans.*, 3885 (2000).
[30] Q.S. Li, P. Yang, H.F. Wang, M.L. Guo. *J. Inorg. Biochem.*, **64**, 181 (1996).
[31] T. Alketa, G. Psomas, C.P. Raptopoulou, V. Psycharis, D.P. Kessissoglou. *Polyhedron*, **28**, 3272 (2009).
[32] Y.M. Song, Q. Wu, P.J. Yang, N.N. Luan, L.F. Wang, Y.M. Liu. *J. Inorg. Biochem.*, **100**, 1685 (2006).
[33] E.C. Long, J.K. Barton. *Acc. Chem. Res.*, **23**, 271 (1990).
[34] G. Psomas. *J. Inorg. Biochem.*, **102**, 1798 (2008).
[35] A. Wolf, G.H. Shimer, Jr., T. Meehan. *Biochemistry*, **26**, 6392 (1987).
[36] C.V. Kumar, J.K. Barton, N.J. Turro. *J. Am. Chem. Soc.*, **107**, 5518 (1985).
[37] J.R. Lakowicz, G. Webber. *Biochemistry*, **12**, 4161 (1973).
[38] L. Bian, L.Z. Li, Q.F. Zhang, J.F. Dong, T. Xu, J.H. Li, J.M. Kong. *Transition Met. Chem.*, **37**, 783 (2012).
[39] J.Z. Lu, Y.F. Du, H.W. Guo, J. Jiang, X.D. Zeng, L.Q. Zang. *J. Coord. Chem.*, **64**, 1229 (2011).
[40] H.W. Guo, J.Z. Lu, Z.G. Ruan, Y.L. Zhang, Y.J. Liu, L.Q. Zang, J. Jiang, J.W. Huang. *J. Coord. Chem.*, **65**, 191 (2012).
[41] A. Rajendran, B.U. Nair. *Biochim. Biophys. Acta*, **1760**, 1794 (2006).
[42] V.I. Ivanov, L.E. Minchenkova, A.K. Schyolkina, A.I. Poletayer. *Biopolymer*, **12**, 89 (1973).
[43] P. Lincoln, E. Tuite, B. Norden. *J. Am. Chem. Soc.*, **119**, 1454 (1997).
[44] P.U. Maheswari, M. Palaniandavar. *J. Inorg. Biochem.*, **98**, 219 (2004).